

The design and virtual screening of thiourea derivatives as a Sirtuin-1 inhibitor

Ruswanto Ruswanto¹, Richa Mardianingrum², Ade Dwi Septian¹, Arry Yanuar³

¹ Department of Pharmacy, Universitas Bakti Tunas Husada, Jl. Mashudi No. 20, Tasikmalaya, West Java, Indonesia

² Department of Pharmacy, Universitas Perjuangan, Jl. PETA No. 177, Tasikmalaya, West Java, Indonesia

³ Faculty of Pharmacy, Universitas Indonesia, Jakarta, Indonesia

Corresponding author: Ruswanto Ruswanto (ruswanto@universitas-bth.ac.id)

Received 14 June 2023 ♦ Accepted 18 September 2023 ♦ Published 16 November 2023

Citation: Ruswanto R, Mardianingrum R, Septian AD, Yanuar A (2023) The design and virtual screening of thiourea derivatives as a Sirtuin-1 inhibitor. *Pharmacia* 70(4): 1335–1344. <https://doi.org/10.3897/pharmacia.70.e108012>

Abstract

The SIRT1 is overexpressed in a number of cancers. As a result, inhibiting SIRT1 may be used as a cancer treatment technique. Modification of 1-benzoyl-3-methylthiourea derivatives was carried out in this study by changing the aromatic side. The designed compounds (**94**) were subjected to in silico docking, pharmacokinetics, and preclinical testing. In the docking sample, the (4-decyl-N-(methylcarbamothioyl)benzamide (**91**), 2-(benzyloxy)-N-(methylcarbamothioyl)benzamide (**93**) and N-(methylcarbamothioyl)-2-naphthamide (**94**) were predicted to display better inhibition of SIRT1, so they were chosen for subsequent molecular dynamic studies. The compound **93** is proposed as a possible anticancer candidate that inhibits SIRT1 based on the screening results from molecular docking, pharmacokinetic predictions, and molecular dynamics.

Keywords

cancer, molecular docking, molecular dynamics, SIRT1, thiourea

Introduction

SIRT1 and SIRT2, which are part of the sirtuin family of enzymes, have been identified as class III histone deacetylases. Sirtuin was originally recognized as a yeast silent information regulator 2 (Sir2) enzyme. So far, researchers have discovered seven mammalian sirtuins (SIRT1 to SIRT7) that play a role in maintaining genomic stability, responding to stress, regulating lifespan, and promoting tumor growth (Bosch-Presegué and Vaquero 2011).

Regarding sequence, SIRT1, which is closest to yeast Sir2, mediates the formation of heterochromatin by histone deacetylation. The significant role in chromatin modulation and epigenetic alteration of histone H1, H3, and H4 is attributed to the deacetylation of specific lysine

residues by SIRT1. SIRT1 also has non-histone protein substrates, including p53, FOXO and Rb. By deacetylating these substrates, SIRT1 has been associated with various physiological functions (Carafa et al. 2019).

It seems that SIRT1 and SIRT2 are involved in the progression of tumors. Elevated levels of SIRT1 have been detected in various cancer types, such as leukemia, lymphoma, skin cancer, breast cancer, liver cancer, stomach cancer, and colorectal cancer. The role of SIRT1 in tumorigenesis depends on the context, and studies examining whether SIRT1 functions as a tumor suppressor have produced inconsistent results. The anticancer effects of small-molecule inhibitors of SIRT1/2 aid the ability of SIRTs to promote tumor growth. Several small molecules have been discovered and suggested as potential treatments for cancer (Lilly 2011), EX-527

(Gertz et al. 2013), splitomicin (Kozako et al. 2014), sirtinol (Park et al. 2016), cambinol (Choi et al. 2013), AGK2 (Ma et al. 2018), suramin (Li et al. 2015), tenovins (Sonnemann et al. 2015), salermide (Carafa et al. 2019), JGB1741 (Tan et al. 2018), UVI5008 (Nebbio et al. 2011) and inauhzinin have all been identified as sirtuin inhibitors. Only four of these drugs (tenovins, cambinol, UVI5008, and inauhzin) have shown anticancer activity in mice models. The discovery of sirtuin inhibitors with SIRT inhibitory mechanisms has therapeutic promise for developing anticancer medicines.

Thiourea is a chemical that is commonly utilized in drug discovery and development. In previous research, synthesis and activity tests were carried out on cancer cells with several derivatives of 1-benzoyl-3-methyl thiourea (Ruswanto et al. 2015). Still, whether this compound works as an inhibitor of sirtuin-1 is not yet known. The present study utilized in-silico methods, including molecular docking and dynamics simulations, to investigate whether derivative compounds of 1-benzoyl-3-methylthiourea can form a stable interaction with sirtuin-1. Furthermore, the research also conducted preclinical virtual experiments, which included examining the absorption, distribution, metabolism, excretion, and toxicity (ADMET) of the compounds, predicting any potential health effects, and determining the MRDD. The synthetic accessibility of the molecules was also predicted. Therefore, this study aims to employ a molecular modeling technique to uncover 1-benzoyl-3-methylthiourea derivatives expected to be employed as anticancer possibilities due to their inhibition of SIRT1.

Materials and methods

Materials

The hardware utilized is a personal computer with the following specifications: Intel(R) Core(TM) i5-8265U CPU @ 1.60GHz (8 CPUs) × 8.00 GB Ram 64-Bit Windows 10 Operating System. The AutodockTools 1.5.6, Marvin-Sketch 21.17.0, Biovia Discovery Studio Visualizer, Amber 2016, and web-based applications such as PDB (Protein Data Bank), ProSA, SwissADME, PreADMET, and pkCSM were utilized.

SIRT1 structure retrieval and assessments

The SIRTUIN-1 enzyme's three-dimensional structure (PDB ID 4I5I), which comes from Homo sapiens, was acquired from the protein database of the Structural Bioinformatics Research Collaborators (<https://www.rcsb.org/structure/4I5I>). The crystal structure analysis of the catalytic domain of SIRT1 in conjunction with nicotinamide adenine dinucleotide (NAD⁺) and an indole compound (an analog of EX527) has revealed a new mechanism of histone deacetylase inhibition, with a resolution of about 2.5 angstroms.

The data was saved in PDB format, and the structural characteristics were evaluated. The stereochemical characteristics of the 3D structure were first explored using

the Ramachandran plot. Additional properties of the 3D structure were studied, and their coherence was validated using the pdbsum and ProSA online interfaces.

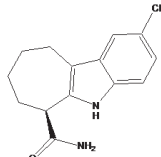
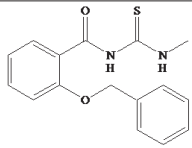
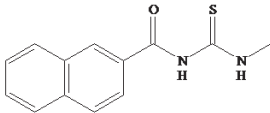
The Ramachandran plot is a valuable tool for illustrating the phi (Φ) and psi (Ψ) dihedral angles of amino acid residues within a protein's structure, identifying the protein structure's allowed and disallowed conformations. The overall consistency and viability of the protein structure are calculated by the ProSA (<https://prosa.services.came.sbg.ac.at/prosa.php>) server. The performance outcomes should fall within the scope of experimentally tested protein structures. The ProSA score determines the Z-score. It demonstrates the protein structure's general coherence and the fold conformations' dependability (Wiederstein and Sippl 2007; Prajapat et al. 2014).

Macromolecule and ligand preparation

The Sirtuin-1 structure was obtained from the PDB with a resolution of 2.5 Å, identified by the PDB ID 4I5I (Zhao et al. 2013; Koushik et al. 2014; Sun et al. 2016; Chi et al. 2019; Wössner et al. 2020). Several structural protein preparations were required before any docking calculations could be conducted. This involves eliminating water molecules and introducing hydrogen atoms. The ligand mode was then used to produce a suitable hypothetical ligand pose called EX527. After that, the EX527 was utilized to dock the potential molecules.

The compound design was carried out from the development of the 1-benzoyl-3-methylthiourea, which had previously been synthesized and tested for its activity on several cancer cells. In this study, the compound was modified by replacing the different groups in the positions on the aromatic ring to become 94 derivative compounds (as in Table 1) so that they would change the lipophilic,

Table 1. Docking results of the three best compounds and the native ligand (EX527).

Compound code	Structure	Binding affinity (kcal/mol)	Inhibition constant
EX527		-9.71	73.09 nM
91		-9.30	153.57 nM
93		-8.76	381.19 nM
94		-8.31	813.74 nM

electronic, and steric parameters. The changes in physico-chemical parameters of the designed compounds can be studied for their activities, and information on groups that play a role in increasing the prediction of their activity on SIRT1 inhibition can be obtained.

The ninety-four of 1-benzoyl-3-methylthiourea derivatives were generated and illustrated in their 2-dimensional form. Subsequently, Marvin Sketch 5.2 software was utilized to conduct geometry optimization. Initially, the ligand was protonated at pH 7.4 to correspond with the pH of human blood in the body. The conformation was assessed to determine the molecular orientation that would be the most stable while interacting with the enzyme's active site. To perform the docking process, the file was saved in two formats, .mrv and .pdb (Ruswanto et al. 2020). The optimized ligand was then used for a further docking study.

In silico pharmacology analysis and pre-clinical trials

Identifying different pharmacological characteristics and bioactivities, a pharmacology study and preclinical experiment were undertaken through web server applications such as SwissADME (<http://www.swissadme.ch/index.php>), <http://pgp.biozyne.com/> and pKCSM (<http://biosig.unimelb.edu.au/pkcsm/>). Furthermore, the PreADMET system was used to forecast the absorption, distribution, and toxicity profiles of 1-benzoyl-3-methylthiourea derivatives (Qidwai et al. 2012). This service computes a drug's pharmacokinetic parameters, such as its intestinal absorption in humans, protein plasma binding, and caco-2 binding. Toxicity parameters were also predicted in silico using the Ames test, rat cancer assay, and mouse cancer assay (Aromatic and Carcinogens 1972).

Synthetic accessibility prediction

The prediction of synthesis accessibility is crucial in determining the feasibility of producing a more optimized medication in a laboratory setting. The SwissADME web interface was employed to evaluate the lead compounds' practicality.

Molecular docking

AutoDockTools 1.5.6 was used to prepare the protein and ligands for docking (The Scripps Research Institute, La Jolla). To prepare the protein for docking, polar hydrogens, and Kollman charges were introduced and saved in .pdbqt format (Morris et al. 2009). Gasteiger charges were computed for the ligands. The specifications were a grid box size of $40 \times 40 \times 40$, coordinates of 42.8139, -21.9161, and 18.4876 (as x, y, and z center of mass, respectively), and spacing of 0.375 Å (Mughtaridi et al. 2019). This sentence means the genetic algorithm was run 100 times, and all the other parameters were left at their default values. AutoDock 4.2 was employed to reproduce the docking process. The AutoDock Tools' interaction determination module was utilized to examine the binding residues and various bonds implicated in the binding of the docked complexes. The resulting

docked complexes were further analyzed using Discovery Studio Visualizer v17.2.0.1634 (BIOVIA, San Diego).

Molecular dynamics simulation

MD simulations were done on 1-benzoyl-3-methylthiourea, which had the lowest binding energy. A single trajectory approach was used to calculate all binding energies using MMGBSA. During the MD simulations, the AMBER ff14SB force field was used for modeling the protein. During the simulation, a general AMBER force field (GAFF) was used for the ligand, and a box with dimensions of $10 \times 10 \times 10$ Å was filled with TIP3P water (Salomon-ferrer et al. 2012). The topology files were generated once the charges of the ligands were balanced using restricted electrostatic potential (RESP). The process of minimization, heating, and equilibration was conducted using the Sander module of Amber 16. The RMSD and RMSF were also determined. The native ligands were utilized as references. The docking and dynamics simulations were performed on a supercomputer equipped with Intel socket LGA1151, PCIE 3.0, good capacitors + Intel i5 Quad cores (4 cores/4 threads; 3.4 GHz) and the latest Kaby Lake processor (Zhang et al. 2003; Qin et al. 2007; Maier et al. 2015).

Results and discussion

SIRT1 structure retrieval and assessments

The sirtuin-1 protein with human origin's 3D structure (4I5I) was obtained from the PDB. Sirtuin-1 has a complex structure involving nicotinamide adenine dinucleotide (NAD⁺), an indole (EX527 analog), and zinc ions. The sirtuin-1 protein structure is composed of 272 amino acids. The three-dimensional structural properties were tested for molecular interaction studies (Fig. 1). Ramachandran



Figure 1. Crystallography structure of SIRT1 (4I5I.pdb).

plots were used to examine the stereochemical characteristics of the structure sirtuin-1 (Fig. 2). In favored and deprived areas, the (<http://www.ebi.ac.uk/thornton-srv/databases/cgi-bin/pdbsum/GetPage.pl?pdbcode=index.html>) server was used to test dihedral angles and a variety of amino acid residues. Sirtuin-1 Ramachandran plots revealed 92.1% in the most preferred region, 7.9% in the authorized regions, and 0% in the banned regions (Zhou et al. 2011; Zhao et al. 2013; De Beer et al. 2014; Erlina and Yanuar 2018; Ruswanto et al. 2018).

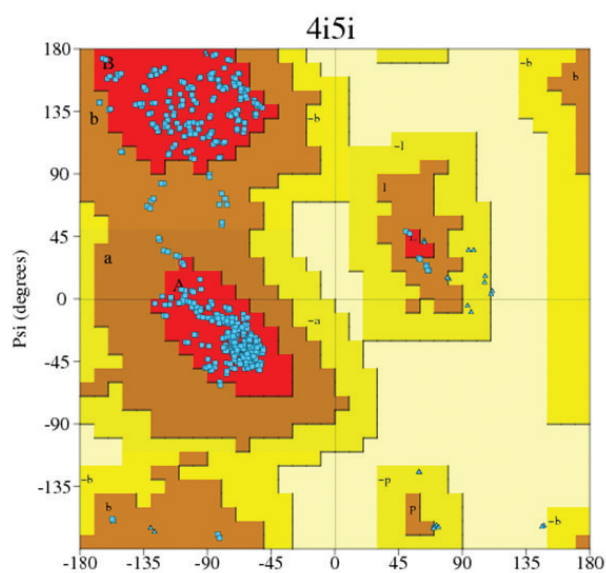


Figure 2. Ramachandran plot.

Fig. 2 displays that the Z-score of the sirtuin-1 structure based on the ProSA score was -8.74, indicating that the Z-score of the sirtuin-1 structure falls within the range of the scores for native protein structures of similar scale. Using the tools indicated above, structure assessments validated the sirtuin-1 protein's good structure quality.

The ProSA program uses C-alpha atoms in a protein structure to calculate Z-scores, which compare the similarity of the structure to known structures of similar size determined by crystallography or NMR. If a model's Z-score is negative, the model has few or no errors. The ProSA web server generated a Z-score of -8.74 for the 4I5I model, which is within the allowed range for similar-sized X-ray and NMR studies. Based on the observations in Fig. 2, the Ramachandran plot statistical data, and the ProSA results presented in Fig. 3, the protein crystallographic structure **4I5I.pdb** has a good quality, stable structure that could be further used in molecular studies.

Docking method validation

Docking method validation was performed with AutoDock software. Docking validation was performed by redocking the natural ligand ((6S)-2-chloro-5,6,7,8,9,10-hexahydro-cyclohepta[b]indole-6-carboxamide, **415**) in the 4I5I.pdb crystallographic structure onto its binding site. The docking process utilized a grid box with dimensions $x = 42.8139 \text{ \AA}$, $y = -21.9161 \text{ \AA}$, and $z = 18.4876 \text{ \AA}$. The parameter used for

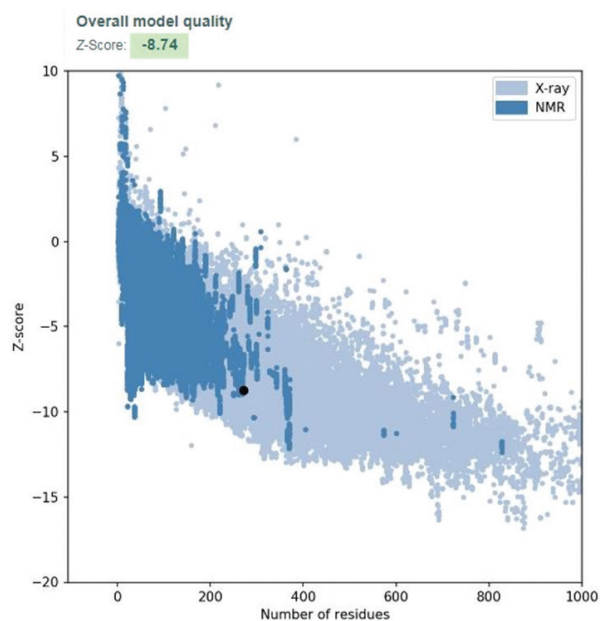


Figure 3. Depiction of the ProSA web interface study of the NMR and X-ray plots of recognised structures in the sirtuin-1 protein structure.

validation was the RMSD, which measures two postures made by comparing the atomic locations of the experimental and docked structures. The method is considered satisfactory if the resulting RMSD value is 2 or lower. The redocking results revealed an RMSD of 0.37 \AA with a binding affinity of -9.71 kcal/mol and an inhibition constant of 75.71 nM . Overlay of the redocking 415 structures with the ones in the crystallographic structure (4I5I.pdb) as shown in Fig. 4 (Wallace et al. 1995; Adelin 2013; Hariono et al. 2020).

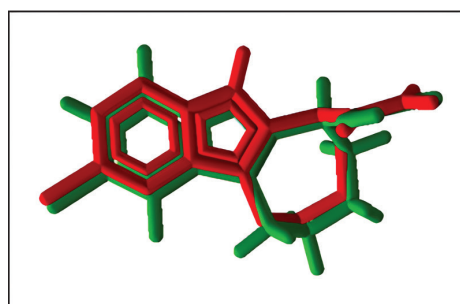


Figure 4. Overlay of the redocked native ligand structure (green) with the crystallographic structure (red).

Docking and visualization results

Molecular interaction studies were conducted on the compounds that target the sirtuin-1 protein. Using AutoDock's molecular docking methods, the generated sirtuin-1 protein structure was docked with the specified chemicals and EX527 (Mardianingrum et al. 2021). AutoDockTools-1.5.6 software was utilized to conduct the docking procedure, and the grid box was the same as that used for the docking validation process. The Gibbs free energy (ΔG) and the strength of the binding affinity between the ligand and

the receptor molecule were calculated due to this docking procedure (Schinkel et al. 1994; Muchtaridi et al. 2019).

From the docking results of the 1-benzoyl-3-methylthiourea derivatives (In Suppl. material 1: tables S1, S2), several compounds that were predicted to have stable interactions were identified as potential anticancer candidates with the sirtuin-1 inhibitor mechanism, as shown in Table 1. Two-dimensional visualization of the compounds can be seen in Figs 5–8.

Due to the low binding affinities and favorable intermolecular interactions of the three compounds in molecular docking analysis, these compounds may be potential candidates for Sirtuin 1 enzyme inhibition in cancer therapy. The compounds' preclinical and pharmacological properties were then assessed.

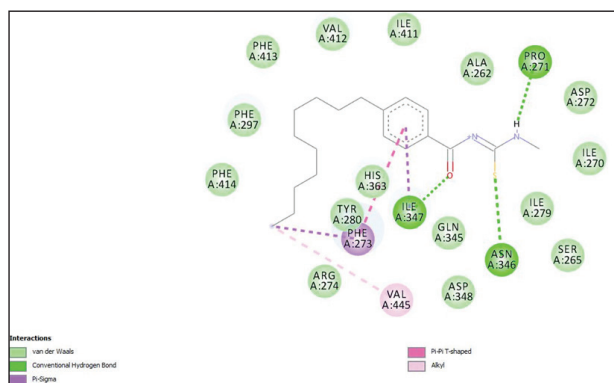


Figure 5. Two-dimensional visualisation of the interactions of compound 91 with SIRT1.

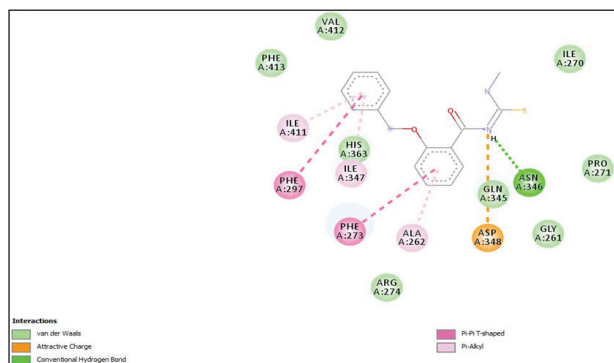


Figure 6. Two-dimensional visualisation of the interactions of compound 93 with SIRT1.

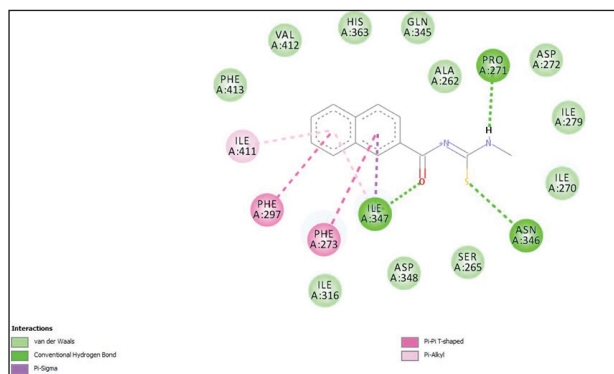


Figure 7. Two-dimensional visualisation of the interactions of compound 94 with SIRT1.

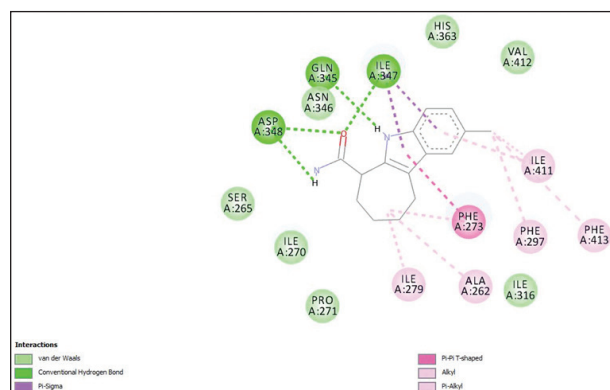


Figure 8. Two-dimensional visualisation of the interactions of the native ligand (EX527) with SIRT1.

Based on the findings in Fig. 5, it can be explained that the interactions that play an important role in its interactions with compound **91-SIRT** complex are three hydrogen bonds (Pro A:271; Asn A:346; Ile A:347) and 15 hydrophobic bonds (Ala A:262; Ser A:265; Ile A:270; Phe A:273; Arg A:274; Ile A:279; Tyr A:280; Phe A:297; Gln A:345; Asp A:348; Ile A:411; Val A:412; Phe A:413; Phe A:414; Val A:445).

Analysis of the 2D visualization of the docking results and the types of interactions comprised by the complex of compound 93-SIRT1 in Fig. 6, it can be explained that there is one hydrogen bond (Asn A:346) and 15 hydrophobic bonds (Gly A:261; Ile A:270; Pro A:271; Phe A:273; Arg A:274; Phe A:297; Gln A:345; Ile A:347; Ala A:348; His A:363; Val A:412; Phe A:413).

For the analysis of the docking results for the compound **94-SIRT1** complex shown in Fig. 7, it can be explained that the stability of the interaction that occurs is due to the presence of three hydrogen bonds (Pro A:271; Asn A:346; Ile A:347) and 11 hydrophobic bonds (Ala A:262; Ser A:265; Ile A:270; Asp A:272; Ile A:279; Ile A:316; Gln A:345; Asp A:348; His A:363; Val A:412; Phe A:413).

While in the EX527-SIRT1 complex, as shown in Fig. 8, there are three hydrogen bonds (Gln A:345; Ile A:347; Asp A:348) and 13 hydrophobic bonds (Ala A:262; Ser A:265; Ile A:270; Pro A:271; Phe A:273; Ile A:279; Phe A:297; Ile A:316; Asn A:346; His A:363; Ile A:411; Val A:412; Phe A:413).

Figs 5–8 shows that the Asn A:346 experienced hydrogen interactions with compounds **91**, **93**, and **94** but not with **EX527**. In contrast, the amino acid residues that experienced hydrophobic interactions with compounds **91**, **93**, **94**, and **EX527** were Phe A:270, Val A:412, and Phe A:413.

In silico preclinical trial and pharmacokinetic prediction

Pharmacokinetic properties and toxicity prediction were evaluated in the earliest preclinical in silico studies of potential inhibitors **91**, **93**, and **94**. To predict the pharmacokinetic properties, preADMET (<http://preadmet.bmdrc.org/>), pkCSM (<http://biosig.unimelb.edu.au/pkcsm/prediction>) and swissadme (<http://www.swissadme.ch/index.php>) interfaces were used. PkCSM can predict the maximum recommended daily dose of a ligand for its development potential as an anticancer agent.

The maximum tolerated dose for both drugs was determined using pkCSM. Compound **91** demonstrated a significant tolerance level, with a recommended tolerable dose of $-0.148 \log \text{ mg/kg/day}$, while the doses for compound **93** and **94** were 0.329 and $0.092 \log \text{ mg/kg/day}$, respectively. The conclusions were based on the highest prescribed beginning dose for phase 1 clinical trials based on 1222 human clinical trial experimental evidence.

Whether the compounds were substrates for P-glycoprotein (P-gp) was another significant factor that was investigated during the preclinical study. P-gp is an efflux transporter that pumps medicines and other substances out of cells and their substrates, explaining why some tumors resist cancer chemotherapy. P-gp has been identified as an important drug carrier, leading to resistance to anticancer medicines such as imatinib, lonafarnib, and taxanes (Chastagner et al. 2015; Lee et al. 2016).

Therefore, using the Biozyne web interface (<http://pgp.biozyne.com/>), we evaluated compounds **91**, **93**, and **94** for whether or not they are P-gp substrates. As shown in Fig. 9, compounds **91**, **93**, and **94** were found to be very likely not substrates for the P-gp protein pump. This indicates that the compounds have a significantly reduced likelihood of being transported out of the cell, leading to maximal effectiveness.

The next step of the computational study examined the compounds' absorption, distribution, and toxicity. The ADMET test was conducted using the preADMET program (Table 2). The in-silico study included using a

web-based tool called PreADMET to predict the absorption, distribution, metabolism, excretion data, and toxicity properties. The tool can be accessed at <http://preadmet.bmdrc.org/> (Lanevskij et al. 2011; Daina et al. 2017; Ruswanto et al. 2017; Shibata et al. 2020).

From Table 2, it can be observed that all compounds **91**, **93**, and **94** had caco-2 cell parameters in the 4–70 nm/s range, putting them in the moderate permeability category, HIA values in the 70–100% range, indicating that they will be well absorbed, and PPB values higher than 90% for ligands **91**, **93** and **94**, meaning that the compounds in this chemical category are strongly bonded and will therefore be poorly distributed. The native ligand and ligands **4** and **5** have PPB values below 90%, indicating that these compounds will be distributed well throughout the body, as they are weakly bound (Lanevskij et al. 2011).

During preclinical research, measuring the hazardous potential of substances is critical. LD50 values were used to determine the acute toxicity of drugs by measuring their relative toxicity according to the standard measurement. The LD50 value of a substance refers to the concentration of the substance that causes death in 50% of the tested animals. The LD50 estimates for compounds **91**, **93**, and **94** were 3.029, 2.627, and 2.56 mol/kg, respectively, based on a rat-tested model of over 10,000 chemical compounds.

The chronic toxicity of the chemicals in rats has been evaluated through oral administration, to determine the minimum effective dose that induces adverse effects. We

Table 2. Data on the predicted adsorption, distribution and toxicity of the compounds.

No	Compound	Pharmacokinetic prediction			Toxicity prediction		
		Caco2 (nm/sec)	% HIA	% PPB	Ames test	Carcino mouse	Carcino rat
1	EX527	21.5866	91.615	87.21	Mutagen	+	-
2	91	45.3267	94.886	100	Mutagen	-	-
3	93	28.9385	94.857	87.952	Mutagen	-	-
4	94	21.6553	94.817	84.541	Mutagen	-	-

Notes: Caco-2 results: low permeability (less than 4), moderate permeability (4–70), and high permeability (more than 70). HIA results: poorly absorbed compounds (0–20%), moderately absorbed compounds (20–70%), and well-absorbed compounds (70–100%). PPB results: strongly bound chemicals (more than 90%), and weakly bound chemicals (less than 80%) (Aromatic and Carcinogens 1972; Pal et al. 2019).

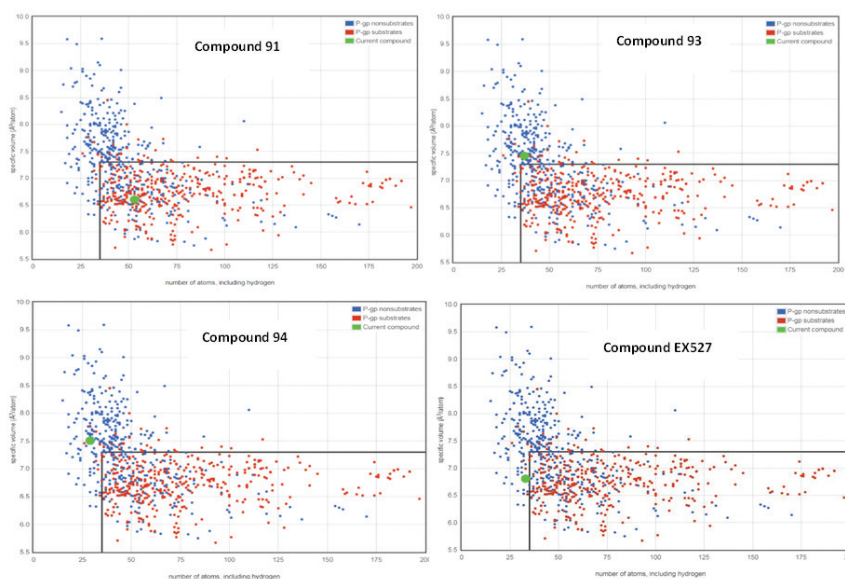


Figure 9. The number of atoms versus the volume of compounds.

discovered that a high concentration of compounds **91** (0.828 log mg/day), **93** (1.325 log mg/day), and **94** (1.078 log mg/day) has no negative effects on rats. The clinical trial conducted using a bioinformatics method indicates that the tested compounds possess the necessary pharmacokinetic qualities for medicine use. Further in vitro and bioassays could be conducted to develop these compounds as effective anticancer drugs.

Synthetic accessibility

Following computer-assisted drug discovery and development, the next stage entails evaluating these compounds in vitro and in vivo bioactivity to identify their potential for development. To evaluate the synthetic feasibility and viability of the compounds, it is important to assess their synthetic accessibility and potential as lead compounds. The prediction is based on the screening and informative research of individual fragment contributions and the refining of structures from a database including millions of previously synthesized molecules. Therefore, it was possible to estimate the compounds' synthetic feasibility through a de novo synthesis approach.

The software called SwissADME was utilized to forecast the synthetic feasibility and effectiveness of the compounds as potential anticancer agents. These techniques can determine the synthetic feasibility percentage by considering the starting materials' complexity and the compounds' structural or residue complexity (Daina et al. 2017). The proposed compounds' synthetic accessibility is presented in Table 3.

The compound will be easy to synthesize if it has a synthetic accessibility value close to 1. The SwissADME analysis suggests that the designed compounds are expected to be easily synthesized, as they all have a score close to 1. In addition, we found that they do not have lead drug likeness.

Molecular dynamics simulation

To evaluate the stability of the interactions that occur in molecular docking, the next step was to carry out MD simulation on the three best compounds (**91**, **93**, and **94** and **EX527**) of

Table 3. Synthetic accessibility analysis of the designed compounds using swissADME.

Compound code	Synthetic accessibility score	Lead likeness
91	2.58	No
93	2.281	No
94	1.55	No

about 94 1-benzoyl-3-methylthiourea derivatives. MD runs of 100,000 ps (100 ns) was carried out on the complexes of **91**, **93**, and **94** compounds with SIRT1. The RMSD of the heavy atoms of SIRT1 over 100 ns can be seen in Fig. 10.

Fig. 10 indicates that all complexes reach a stable conformation after 15 ns. The compound **93**-SIRT1 complex was found to be the most stable in terms of conformation. A plot depicting the RMSF of amino acid residues over 100 ns was generated, as shown in (Fig. 11), to assess the residues' flexibility.

The residual movement patterns were similar among all the complexes, as indicated by the RMSF outcomes. According to the analysis, the protein's amino and carbon terminals displayed significant flexibility, whereas most residues exhibited tight flexibility. The amino acid residues that had the highest fluctuation were ARG274 and CYS374, while the amino acid residues of VAL258 and ILE437 had the lowest fluctuation. This suggests that the binding of the ligand did not cause a significant change in protein conformation.

The compound **93**-SIRT1 complex trajectory was visualized to observe the ligand's position and analyze its interaction. The visualization of their trajectory is shown in Fig. 12.

From Fig. 12, it can be seen that there are changes and movements of compound **93** in the SIRT1 that occur during the dynamic molecular simulation process. When comparing the initial state of the amino acid residues at the beginning of the simulation to the final state at the end of the simulation, it can be seen that there is a change in the shape of the amino acid residue, especially between the ILE279-PHE287 residues (as in the green circle).

MMGBSA calculations were performed to assess the binding affinity of each compound for SIRT1, and the results were presented in (Table 4).

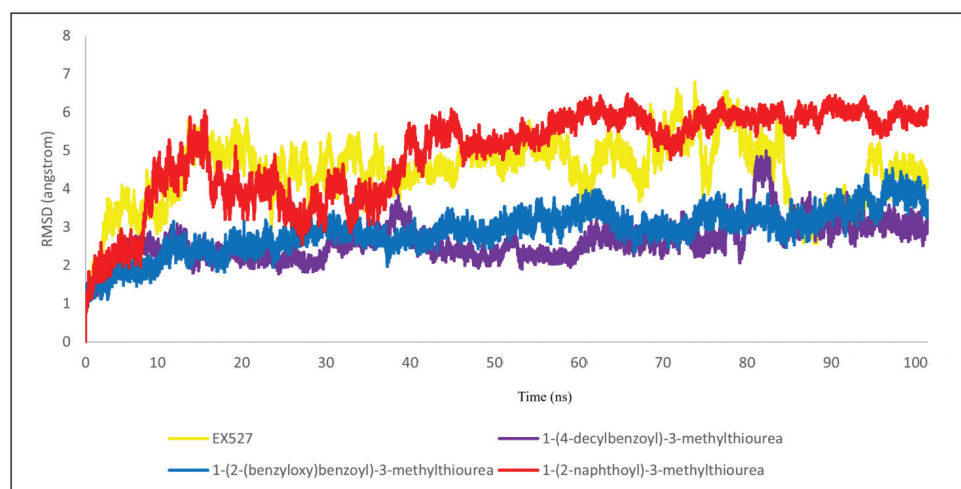


Figure 10. The root mean square deviation (RMSD) value of each ligand-SIRT1 complex during 50-ns dynamics runs calculated from heavy atoms of the protein for compounds **91** (purple), **93** (blue), **94** (red) and **EX527** (yellow).

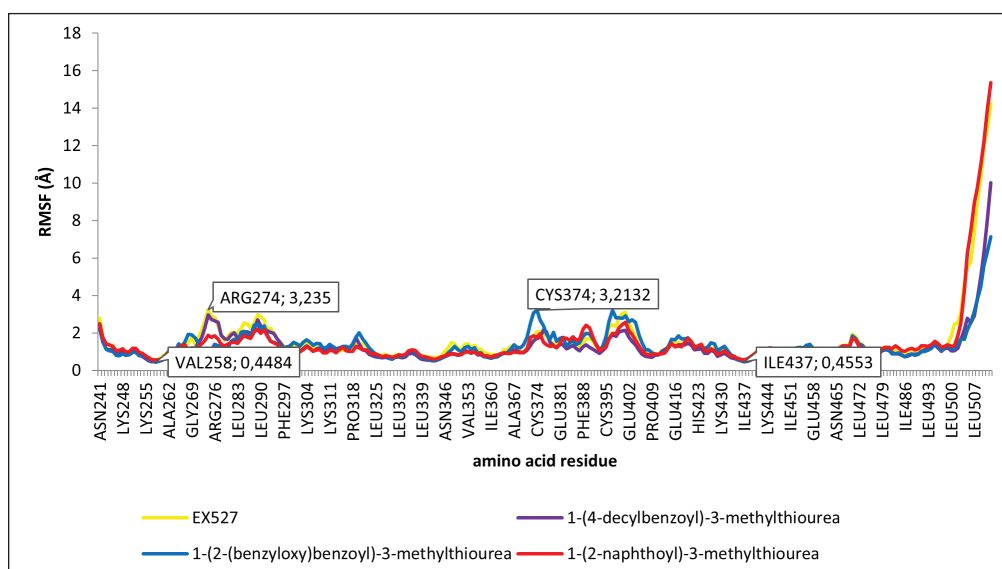


Figure 11. The RMSF plot of each amino acid residue during 100-ns dynamics simulation.

Table 4. The MMGBSA energy was used to break down the calculated binding energies.

Energy component	System			
	EX527-SIRT1	Comp. 91-SIRT1	Comp. 93-SIRT1	Comp. 94-SIRT1
V_{dw}	-20.15±3.40	-53.49±4.92	-60.28±3.51	-27.39±4.39
EEL	16.65±27.24	18.59±19.91	-49.79±23.53	0.97±20.78
E_{GB}	-12.64±25.98	-1.16±17.97	25.59±22.92	3.36±18.46
E_{SUR}	-2.08±0.32	-6.39±0.54	-5.14±0.16	-3.17±0.45
ΔG_{gas} (VdW+EEL)	-3.49±28.19	-34.91±22.38	-110.07±23.15	-26.43±20.92
ΔG_{solv} (EGB + ESURF)	-14.72±25.89	-7.55±17.68	20.45±22.92	0.18±18.49
ΔG_{MMGBSA}	-18.21±4.49	-42.45±7.67	-89.62±8.54	-26.25±5.93

* kcal/mol.

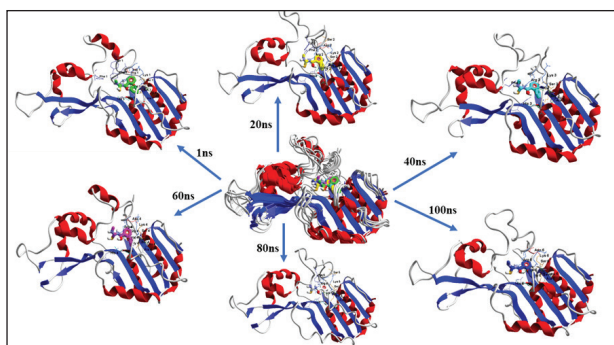


Figure 12. The trajectory of compound 93 against SIRT1.

Compound **93** demonstrated a stronger intermolecular interaction with SIRT1 than other ligands, indicating that it formed more interactions with the receptor than compound **91**, compound **94**, and EX527. Van der Waals and electrostatic energies between compounds and receptors were calculated to measure their interactions. This was further supported by the observation that compound **93** had more surrounding residues and produced more hydrogen bonds (according to the hydrogen bond analysis) than the

other ligands, indicating stronger interaction with SIRT1. However, the structure of compound **93** is larger than the others, leading to better van der Waals interactions. Most of the binding site residues were discovered to be hydrophobic amino acids. Furthermore, compound **93** has a reduced binding energy to the SIRT1 receptor -89.62 ± 8.54 kcal/mol) than the others suggest that compound **93** prefers to bind SIRT1, so it could be recommended as a potential anticancer candidate drug to inhibit SIRT1.

Conclusions

Based on the results of virtual screening through docking, pharmacokinetics prediction, preclinical trial predictions, and molecular dynamics, compound **93** was the best potential anticancer candidate drug through the inhibition of SIRT1.

The positive findings of this work could serve as a foundation for future oncology research, specifically addressing SIRT1 inhibitors. Advanced clinical trials, exploring structural variations, mechanistic studies, and synergistic effects with other therapies are some of the prospective avenues and opportunities.

Acknowledgements

This research was funded by the Penelitian Pasca Doktor Grant (Nomor: NKB-2964/UN2.RST/HKP.05.00/2020) from the Ministry of Research and Technology/BRIN Indonesia. We appreciate the facilities at STIKes Bakti Tunas Husada and Universitas Perjuangan Tasikmalaya.

Conflict of interest

The authors do not have any competing interests to disclose.

References

- Adelin T (2013) Penambatan molekuler kurkumin dan analognya pada enzim siklooksigenase-2. *Jurnal Medika Veterinaria* 7(1): 30–34.
- Aromatic O, Carcinogens A (1972) Carcinogens as frameshift mutagens: metabolites and derivatives of 2-acetylaminofluorene and other aromatic amine carcinogens. *PNAS* 69(11): 3128–3132. <https://doi.org/10.1073/pnas.69.11.3128>
- De Beer TAP, Berka K, Thornton JM, Laskowski RA (2014) PDBsum additions. *Nucleic Acids Research* 42: 292–296. <https://doi.org/10.1093/nar/gkt940>
- Bosch-Presegué L, Vaquero A (2011) The dual role of sirtuins in cancer. *Genes & Cancer* 2: 648–662. <https://doi.org/10.1177/1947601911417862>
- Carafa V, Altucci L, Nebbioso A (2019) Dual tumor suppressor and tumor promoter action of sirtuins in determining malignant phenotype. *Frontiers in Pharmacology* 10: 1–14. <https://doi.org/10.3389/fphar.2019.00038>
- Chastagner P, Sudour H, Mriouah J, Barberi-Heyob M, Bernier-Chastagner V, Pinel S (2015) Preclinical studies of pegylated- and non-pegylated liposomal forms of doxorubicin as radiosensitizer on orthotopic high-grade glioma xenografts. *Pharmaceutical Research* 32: 158–166. <https://doi.org/10.1007/s11095-014-1452-x>
- Chi S, Ohue M, Gryniukov A, Borysko P, et al. (2019) A prospective compound screening contest identified broader inhibitors for Sirtuin 1. *Scientific Reports* 9: 19585. <https://doi.org/10.1038/s41598-019-55069-y>
- Choi G, Lee J, Ji JY, Woo J, Kang NS, Cho SY, Kim HR, Ha JD, Han S-Y (2013) Discovery of a potent small molecule SIRT1/2 inhibitor with anticancer effects. *International Journal of Oncology* 43(4): 1205–1211. <https://doi.org/10.3892/ijo.2013.2035>
- Daina A, Michielin O, Zoete V (2017) SwissADME: a free web tool to evaluate pharmacokinetics, drug-likeness and medicinal chemistry friendliness of small molecules. *Scientific Reports* 7: 42717 <https://doi.org/10.1038/srep42717>
- Erlina L, Yanuar A (2018) Molecular dynamics simulation of SIRT1 inhibitor from Indonesian herbal database. *Journal of Young Pharmacists* 10(1): 3–6. <https://doi.org/10.5530/jyp.2018.10.2>
- Gertz M, Fischer F, Thi G, Nguyen T, Lakshminarasimhan M, Schutkowski M, Weyand M, Steegborn C (2013) Ex-527 inhibits Sirtuins by exploiting their unique NAD⁺-dependent deacetylation mechanism. *PNAS* 110(30): E2772–E2781. <https://doi.org/10.1073/pnas.1303628110>
- Hariono M, Nuwarda RF, Yusuf M, Rollando R, Jenie RI, Al-Najjar B, Julianus J, Putra KC, Nugroho ES, Wisnumurti YK, Dewa SP, Jati BW, Tiara R, Ramadani RD, Qodria L, Wahab HA (2020) Arylamide as potential selective inhibitor for matrix metalloproteinase 9 (MMP9): design, synthesis, biological evaluation, and molecular modeling. *Journal of Chemical Information and Modeling* 60: 349–359. <https://doi.org/10.1021/acs.jcim.9b00630>
- Koushik V, Alvala M, Saketh D, Viswanadha S, Sriram D, Yogeewari P (2014) Structure-based drug design of small molecule SIRT1 modulators to treat cancer and metabolic disorders. *Journal of Molecular Graphics and Modelling* 52: 46–56. <https://doi.org/10.1016/j.jmgm.2014.06.005>
- Kozako T, Suzuki T, Yoshimitsu M, Arima N, Honda S, Soeda S (2014) Anticancer agents targeted to sirtuins. *Molecules* 19(12): 20295–20313. <https://doi.org/10.3390/molecules191220295>
- Lanevskij K, Dapkunas J, Juska L, Japertas P, Didziapetris R (2011) QSAR analysis of blood – brain distribution: the influence of plasma and brain tissue binding. *Journal of Pharmaceutical Sciences* 100(6): 2147–2160. <https://doi.org/10.1002/jps.22442>
- Lee HN, Jang HY, Kim HJ, Shin SA, Choo GS, Park YS, Kim SK, Jung JY (2016) Antitumor and apoptosis-inducing effects of α -mangostin extracted from the pericarp of the mangosteen fruit (*Garcinia mangostana* L.) in YD-15 tongue mucoepidermoid carcinoma cells. *International Journal of Molecular Medicine* 37(4): 939–948. <https://doi.org/10.3892/ijmm.2016.2517>
- Li H, Li H, Qu H, Zhao M, Yuan B, Cao M, Cui J (2015) Suramin inhibits cell proliferation in ovarian and cervical cancer by downregulating heparanase expression. *Cancer Cell International* 15: 1–11. <https://doi.org/10.1186/s12935-015-0196-y>
- Lilly E (2011) Sirtuin 1 (SIRT1): The Misunderstood HDAC. *SLAS Discovery* 16(10): 1153–1169. <https://doi.org/10.1177/1087057111422103>
- Ma W, Zhao X, Wang K, Liu J, Huang G (2018) Dichloroacetic acid (DCA) synergizes with the SIRT2 inhibitor Sirtinol and AGK2 to enhance anti-tumor efficacy in non-small cell lung cancer. *Cancer Biology & Therapy* 19: 835–846. <https://doi.org/10.1080/15384047.2018.1480281>
- Maier JA, Martinez C, Kasavajhala K, Wickstrom L, Hauser K, Simmerling C (2015) ff14SB: Improving the accuracy of protein side chain and backbone parameters from ff99SB. *Journal of Chemical Theory and Computation* 11(8): 3696–3713. <https://doi.org/10.1021/acs.jctc.5b00255>
- Mardianingrum R, Endah SRN, Suhardiana E, Ruswanto R, Siswandono S (2021) Docking and molecular dynamic study of isoniazid derivatives as anti-tuberculosis drug candidate. *Chemical Data Collections* 32: 100647. <https://doi.org/10.1016/j.cdc.2021.100647>
- Morris GM, Huey R, Lindstrom W, Sanner MF, Belew RK, Goodsell DS, Olson AJ (2009) AutoDock4 and AutoDockTools4: automated docking with selective receptor flexibility. *Software News and Updates* 30(16): 2785–2791. <https://doi.org/10.1002/jcc.21256>
- Muchtaridi M, Yusuf M, Syahidah HN, Subarnas A, Zamri A, Bryant SD, Langer T (2019) Cytotoxicity of chalcone of eugenia aquea burm F. leaves against T47D breast cancer cell lines and its prediction as an estrogen receptor antagonist based on pharmacophore-molecular dynamics simulation. *Advances and Applications in Bioinformatics and Chemistry* 12: 33–43. <https://doi.org/10.2147/AABC.S217205>
- Nebbioso A, Pereira R, Khanwalkar H, Matarese F, García-Rodríguez J, Miceli M, Logie C, Kedinger V, Ferrara F, Stunnenberg HG, de Lera AR, Gronemeyer H, Altucci L (2011) Death receptor pathway activation and increase of ROS production by the triple epigenetic inhibitor UVI5008. *Molecular Cancer Therapeutics* 10(12): 2394–2404. <https://doi.org/10.1158/1535-7163.MCT-11-0525>
- Pal S, Kumar V, Kundu B, Bhattacharya D, Preethy N, Reddy MP, Talukdar A (2019) Ligand-based pharmacophore modeling, virtual screening and molecular docking studies for discovery of potential topoisomerase I inhibitors. *Computational and Structural Biotechnology Journal* 17: 291–310. <https://doi.org/10.1016/j.csbj.2019.02.006>
- Park EY, Woo Y, Kim SJ, Kim DH, Lee EK, De U, Kim KS, Lee J, Jung JH, Ha K, Choi WS, Kim IS, Lee BM, Yoon S, Moon HR, Kim HS (2016) Anticancer effects of a new SIRT inhibitor, MHY2256, against human breast cancer MCF-7 cells via regulation of MDM2-p53 binding. *International Journal of Biological Sciences* 12(12): 1555–1567. <https://doi.org/10.7150/ijbs.13833>
- Prajapat R, Marwal A, Gaur RK (2014) Recognition of errors in the refinement and validation of three-dimensional structures of AC1 proteins of begomovirus strains by using ProSA-Web. *Journal of Viruses* 2014: 752656. <https://doi.org/10.1155/2014/752656>

- Qidwai T, Yadav DK, Khan F, Dhawan S, Bhakuni RS (2012) QSAR, docking and ADMET studies of artemisinin derivatives for anti-malarial activity targeting plasmepsin II, a hemoglobin-degrading enzyme from *P. falciparum*. *Current Pharmaceutical Design* 18(37): 6133–6154. <https://doi.org/10.2174/138161212803582397>
- Qin Z, Kastrati I, Chandrasena REP, Liu H, Yao P, Petukhov PA, Bolton JL, Thatcher GRJ (2007) Benzothioephene selective estrogen receptor modulators with modulated oxidative activity and receptor affinity. *Journal of Medicinal Chemistry* 50(11): 2682–2692. <https://doi.org/10.1021/jm070079j>
- Ruswanto, Miftah AM, Tjahjono DH, Siswandono (2015) Synthesis and in vitro cytotoxicity of 1-benzoyl-3-methyl thiourea derivatives. *Procedia Chemistry* 17: 157–161. <https://doi.org/10.1016/j.proche.2015.12.105>
- Ruswanto, Siswandono, Richa M, Tita N, Tresna L (2017) Molecular docking of 1-benzoyl-3-methylthiourea as anti cancer candidate and its absorption, distribution, and toxicity prediction. *Journal of Pharmaceutical Sciences and Research* 9(5): 680–684.
- Ruswanto R, Mardianingrum R, Siswandono S, Kesuma D (2020) Reverse docking, molecular docking, absorption, distribution, and toxicity prediction of artemisinin as an anti-diabetic candidate. *Molekul* 15: 88–96. <https://doi.org/10.20884/1.jm.2020.15.2.579>
- Ruswanto R, Garna IM, Tuslinah L, Mardianingrum R, Lestari T, Nofianti T (2018) Kuersetin, penghambat uridin 5-monofosfat sintase sebagai kandidat anti-kanker. *ALCHEMY Jurnal Penelitian Kimia* 14(2): 236–252. <https://doi.org/10.20961/alchemy.14.2.14396.236-254>
- Salomon-ferrer R, Case DA, Walker RC (2013) An overview of the Amber biomolecular simulation package. *WIREs Computational Molecular Science* 3(2): 198–210. <https://doi.org/10.1002/wcms.1121>
- Schinkel AH, Smit JJM, van Tellingen O, Beijnen JH, Wagenaar E, van Deemter L, Mol CAAM, der Valk MA, Robanus-Maandag EC, Riele HPJ, Berns AJM, Borst P (1994) Disruption of the mouse *m* & *la* P-glycoprotein gene leads to a deficiency in the blood-brain barrier and to increased sensitivity to drugs. *Cell* 77(4): 491–502. [https://doi.org/10.1016/0092-8674\(94\)90212-7](https://doi.org/10.1016/0092-8674(94)90212-7)
- Shibata T, Yamagata T, Kawade A, Asakura S, Toritsuka N, Koyama N, Hakura A (2020) Evaluation of acetone as a solvent for the Ames test. *Genes and Environment* 42: 1–8. <https://doi.org/10.1186/s41021-020-0143-6>
- Sonnemann J, Kahl M, Siranjeevi PM, Blumrich A, Blümel L, Becker S, Wittig S, Winkler R, Krämer OH, Beck JF (2015) Reverse chemomodulatory effects of the SIRT1 activators resveratrol and SRT1720 in Ewing's sarcoma cells: resveratrol suppresses and SRT1720 enhances etoposide – and vincristine – induced anticancer activity. *Journal of Cancer Research and Clinical Oncology* 142: 17–26. <https://doi.org/10.1007/s00432-015-1994-2>
- Sun Y, Zhou H, Zhu H, Leung S (2016) Ligand-based virtual screening and inductive learning for identification of SIRT1 inhibitors in natural products. *Scientific Reports* 6: 19312. <https://doi.org/10.1038/srep19312>
- Tan YJ, Lee YT, Yeong KY, Petersen SH, Kono K, Tan SC, Oon CE (2018) Anticancer activities of a benzimidazole compound through sirtuin inhibition in colorectal cancer. *Future Medicinal Chemistry* 10(17). <https://doi.org/10.4155/fmc-2018-0052>
- Wallace AC, Laskowski RA, Thornton JM (1995) LIGPLOT: a program to generate schematic diagrams of protein-ligand interactions *Clean up structure. Protein Engineering, Design and Selection* 8(2): 127–134. <https://doi.org/10.1093/protein/8.2.127>
- Wiederstein M, Sippl MJ (2007) ProSA-web: interactive web service for the recognition of errors in three-dimensional structures of proteins. *Nucleic Acids Research* 35(suppl_2): W407–W410. <https://doi.org/10.1093/nar/gkm290>
- Wössner N, Alhalabi Z, González J, Swyter S, Gan J, Sippl W, Jung M (2020) Sirtuin 1 inhibiting thiocyanates (S1th) – A new class of isotype selective inhibitors of NAD + dependent lysine deacetylases. *Frontiers in Oncology* 10: 1–15. <https://doi.org/10.3389/fonc.2020.00657>
- Zhang WEI, Yang R, Cieplak P, Luo RAY, Lee T, Caldwell J, Wang J, Kollman P (2003) A point-charge force field for molecular mechanics simulations of proteins based on condensed-phase. *Journal of Computational Chemistry* 24(16): 1999–2012. <https://doi.org/10.1002/jcc.10349>
- Zhao X, Allison D, Condon B, Zhang F, Gheyti T, Zhang A, Ashok S, Russell M, Macewan I, Qian Y, Jamison JA, Luz JG (2013) The 2.5 Å crystal structure of the SIRT1 catalytic domain bound to nicotinamide adenine dinucleotide (NAD +) and an indole (EX527 analogue) reveals a novel mechanism of histone deacetylase inhibition. *Journal of Medicinal Chemistry* 56(3): 963–969. <https://doi.org/10.1021/jm301431y>
- Zhou AQ, Hern CSO, Regan L (2011) Revisiting the Ramachandran plot from a new angle. *Protein Science* 20(7): 1166–1171. <https://doi.org/10.1002/pro.644>

Supplementary material 1

The structure and docking results of the 1-benzoyl-3-methylthioureas derivatives

Authors: Ruswanto Ruswanto, Richa Mardianingrum, Ade Dwi Septian, Arry Yanuar

Data type: pdf

Copyright notice: This dataset is made available under the Open Database License (<http://opendatacommons.org/licenses/odbl/1.0>). The Open Database License (ODbL) is a license agreement intended to allow users to freely share, modify, and use this Dataset while maintaining this same freedom for others, provided that the original source and author(s) are credited.

Link: <https://doi.org/10.3897/pharmacia.70.e108012.suppl1>